Contribution from the Department of Chemistry,
University of Houston, Houston, Texas 77004

Reaction of $Rh_2(O_2CCH_3)_4$ with *N*-Phenylacetamide: Substitution Products and Geometric Isomers

R. S. Lifsey, X. Q. Lin, M. Y. Chavan, M. Q. Ahsan, K. M. Kadish,* and J. L. Bear*

Received August 19, 1986

The products from the reaction of $Rh_2(O_2CCH_3)_4$ with *N*-phenylacetamide, $PhNHOCCH_3$, were isolated by high-performance liquid chromatography and characterized by mass spectrometry, ^{13}C NMR spectroscopy, and electronic absorption spectroscopy. These results indicate that 7 out of 12 possible products with the general formula $Rh_2(O_2CCH_3)_n(PhNOCCH_3)_{4-n}$ were formed. Formation constants for mono- and bis(dimethyl sulfoxide) adducts of each complex were determined in methylene chloride by using spectrophotometric methods. Half-wave potentials for the oxidation of each complex were also determined in methylene chloride (CH_2Cl_2) and dimethyl sulfoxide (Me_2SO). Two $Rh_2(PhNOCCH_3)_4$ isomers were investigated in detail and showed significant isomer effects in both the formation constants for Me_2SO addition and the electronic absorption spectra. Isomer **8** formed a bis(dimethyl sulfoxide) adduct while isomer **7** was capable of forming only a monoadduct. The two geometric isomers of $Rh_2(O_2CCH_3)(PhNOCCH_3)_3$ exhibited a smaller isomer effect in the formation constants and spectra. Crystal and molecular structures of the two tetrakis(*N*-phenylacetamidate) isomers $Rh_2(PHNOCCH_3)_4(Me_2SO)_2$ (**8**(Me_2SO)$_2$) and Rh_2-$(PhNOCCH_3)_4(Me_2SO)$ (**7**(Me_2SO)) were determined by single-crystal X-ray diffraction techniques. The bis(dimethyl sulfoxide) adduct of **8** crystallizes as blood red tabular crystals in the orthorhombic space group $Pna2_1$ with four formula weights in the unit cell of dimensions a = 15.780 (4) Å, b = 11.170 (5) Å, and c = 21.212 (4) Å with a final convergence to R = 0.027 and R_w = 0.031. The four equatorial positions of each rhodium are occupied by two N and two O atoms cis to their own kind. The two axial positions are occupied by Me_2SO bound through the sulfur atoms. The two Rh–S bond lengths are 2.606 (2) and 2.566 (2) Å, and the Rh–Rh distance is 2.448 (1) Å. The mono(dimethyl sulfoxide) adduct of **7** crystallizes as a deep aquamarine block in the triclinic $P\bar{1}$ space group with two formula weights in the unit cell of dimensions a = 8.333 (8) Å, b = 13.069 (4), and c = 17.641 (7) Å with a final convergence to R = 0.038 and R_w = 0.440. One rhodium is bound to three N's and one O in the basal plane whereas the second rhodium is bound equatorially to three O's and one N. One Me_2SO is bound axially via its S atom to the rhodium with three equatorial oxygens, and the axial site of the second rhodium is not occupied. The Rh–Rh and Rh–S bond distances for **7**(Me_2SO) are 2.397 (1) and 2.395 (1) Å, respectively, and are considerably shorter than those found for the bis(dimethyl sulfoxide) adduct of compound **8**.

Introduction

During the last 20 years a number of different dirhodium(II) carboxylates have been synthesized and characterized.[1] There are now also numerous reports of dirhodium(II) complexes that contain bridging donor atoms other than oxygen.[2-10] Studies of these compounds have shown that complexes containing mixed hetero donor atoms in the basal plane are far more complex with respect to their electronic and/or structural effects than dirhodium(II) carboxylates.

Our own laboratory has synthesized and carried out chemical and electrochemical studies on mixed carboxylate- and amidate-bridged dirhodium complexes of the general formula Rh_2-$(O_2CCH_3)_n(RNOCR')_{4-n}$ (where R = H, C_6H_5, R' = CH_3, CF_3, and n = 0–3).[5-10,13,14] As seen in Figure 1, there are 14 possible substitution products comprised of isomers (12 geometric and two optical) for various values of n. The number of isomers actually formed in the exchange of amidate for acetate is considerably less than the total possible number. For example, the reaction of $Rh_2(O_2CCH_3)_4$ with acetamide produces six products.[10] These products include I, IIa, IIc, IId, IIIa, and IVa in Figure 1. Only one isomer of the tris(acetamidate)- and tetrakis(acetamidate)-substituted complexes is formed. This selectivity suggests that the only exchange that occurs is one involving acetamidate and acetate and that the addition of each acetamidate bridge to the dirhodium complex has a directing influence on the following substitution reaction.

The equatorial ligand field of the complexes depends on the number of hetero binding ligands and on their bonding geometry. The effect of changes in the ligand field on either local or overall point group symmetry is reflected in a number of factors. These include the electronic and molecular structure of the rhodium dimers, the Rh–Rh bond polarization, and the chemistry that occurs at the axial position(s) of a given dirhodium complex. The $Rh_2(O_2CCH_3)_n(HNOCCH_3)_{4-n}$ system cannot be used to investigate isomer effects since only one isomer of the tris- and tetrakis(acetamidate) complexes is formed. The bis-substituted complex is present in three geometric forms, but these isomers could not be separated on a preparative-LC scale.

We previously reported the isolation of two $Rh_2(PhNOCCH_3)_4$ geometric isomers from the reaction of $Rh_2(O_2CCH_3)_4$ and *N*-phenylacetamide.[7] Since then we have investigated the geometric isomer distribution among all the different substitution products. In this paper we report the results of this investigation. We also report formation constants for Me_2SO addition to each geometric isomer of the four substitution products involving *N*-phenylacetamide as well as the electrochemical properties and the electronic absorption spectra of each complex. In addition, the crystal and molecular structures for Me_2SO adducts of two $Rh_2(PhNOCCH_3)_4$ geometric isomers are described.

Experimental Section

Reagents. $Rh_2(O_2CCH_3)_4$ was purchased from Matthey Bishop, Inc., Malvern, PA. *N*-Phenylacetamide was obtained from Aldrich Chemical Co., Milwaukee, WI, and was used without further purification. All solvents were of reagent grade or HPLC grade quality.

Preparation of $Rh_2(O_2CCH_3)_n(PhNOCCH_3)_{4-n}$, n = 0–4. One gram (2.26 mmol) of $Rh_2(O_2CCH_3)_4$ was mixed with 30.0 g (0.222 mol) of *N*-phenylacetamide in a 100-mL round-bottom flask. The flask was evacuated, sealed with a stopcock, placed in an oil bath, and heated at 128–135 °C while the reaction mixture was magnetically stirred. Every 24 h, an aliquot of the reaction mixture was chromatographed and the relative ratio of the reaction products was determined. The reaction was stopped after 96 h, at which time sufficient amounts of each product were present for separation. Excess *N*-phenylacetamide was then removed by sublimation. All products were separated and purified by HPLC, and the parent mass of each compound was determined by using liquid

(1) Felthouse, T. R. *Prog. Inorg. Chem.* **1982**, *29*, 73 and references therein.
(2) Cotton, F. A.; Felthouse, T. R. *Inorg. Chem.* **1981**, *20*, 584.
(3) Cotton, F. A.; Han, S.; Wang, W. *Inorg. Chem.* **1984**, *23*, 4762.
(4) Tocher, D. A.; Tocher, J. H. *Inorg. Chim. Acta* **1985**, *104*, L15.
(5) Dennis, A. M.; Howard, R. A.; Lancon, D.; Kadish, K. M.; Bear, J. L. *J. Chem. Soc., Chem. Commun.* **1982**, 339.
(6) Kadish, K. M.; Lancon, D.; Dennis, A. M.; Bear, J. L. *Inorg. Chem.* **1982**, *21*, 2987.
(7) Duncan, J.; Malinski, T.; Zhu, T. P.; Hu, Z. S.; Kadish, K. M.; Bear, J. L. *J. Am. Chem. Soc.* **1982**, *104*, 5507.
(8) Bear, J. L.; Zhu, T. P.; Malinski, T.; Dennis, A. M.; Kadish, K. M. *Inorg. Chem.* **1984**, *23*, 674.
(9) Zhu, T. P.; Ahsan, M. Q.; Malinski, T.; Kadish, K. M.; Bear, J. L. *Inorg. Chem.* **1984**, *23*, 2.
(10) Chavan, M. Y.; Zhu, T. P.; Lin, X. Q.; Ahsan, M. Q.; Bear, J. L.; Kadish, K. M. *Inorg. Chem.* **1984**, *23*, 4538.
(11) Blakley, C. R.; Carmody, J. J.; Vestal, M. L. *J. Am. Chem. Soc.* **1980**, *102*, 5931.
(12) Germain, G.; Main, P.; Woolfson, M. M. *Acta Crystallogr., Sect. A: Cryst. Phys., Diffr., Theor. Gen. Crystallogr.* **1971**, *A27*, 368.
(13) Ahsan, M. Q.; Bernal, I.; Bear, J. L. *Inorg. Chem.* **1986**, *25*, 260.
(14) Chavan, M. Y.; Lin, X. Q.; Ahsan, M. Q.; Bernal, I.; Bear, J. L.; Kadish, K. M. *Inorg. Chem.* **1986**, *25*, 1281.

0020-1669/87/1326-0830$01.50/0

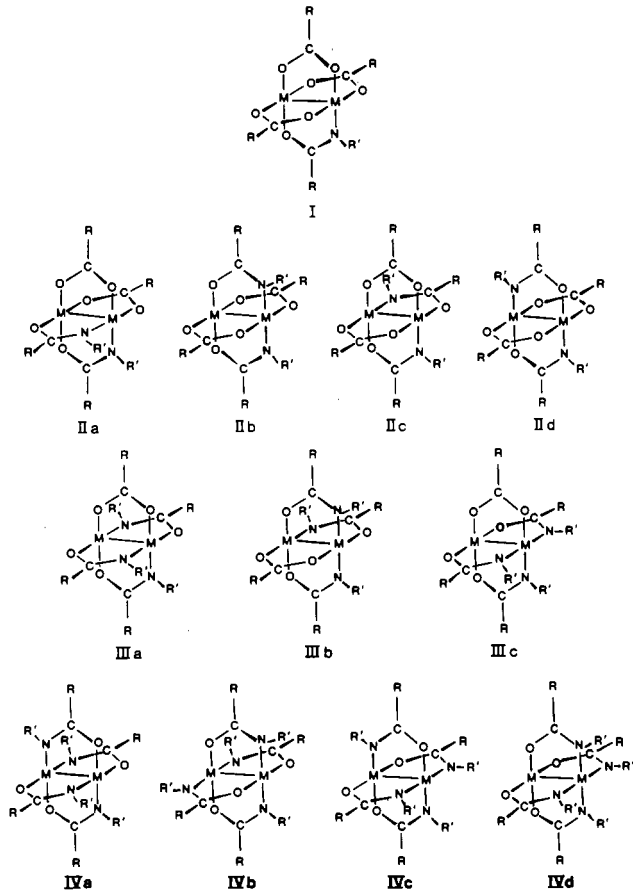

Figure 1. Structures of the possible geometric isomers of the four substitution products in the exchange of bridging ligands. R = CH_3, and R′ = C_6H_5.

chromatography–mass spectrometry (LC–MS) operating in the negative-ion mode.

Separation of Dirhodium(II) Complexes. A Waters Associates high-performance liquid chromatographic (HPLC) system was used in the separation procedure. The system consisted of a Model 6000A solvent delivery system, a Model U6-K injector, a Model 440 variable-wavelength UV detector set at 546 nm, and an RCM-100 radial compression module containing a 10-μm Radial-Pak CN column. The mobile phase was high-purity HPLC-grade methanol. The reaction mixtures were dissolved in methanol and injected (500–1000 μL/injection), after which each band was collected. $Rh_2(O_2CCH_3)_n(PhNOCCH_3)_{4-n}$ compounds having larger *n* values elute first. In this paper, the isomer of each $Rh_2(O_2CCH_3)_n(PhNOCCH_3)_{4-n}$ complex is identified by its band number in the HPLC separation which is shown in Figure 2. The numbered bands are as follows: (**1**) $Rh_2(O_2CCH_3)_4$; (**2**) $Rh_2(O_2CCH_3)_3(PhNOCCH_3)$; (**3** and **4**) $Rh_2(O_2CCH_3)_2(PhNOCCH_3)_2$; (**5** and **6**) $Rh_2(O_2CCH_3)(PhNOCCH_3)_3$; (**7** and **8**) $Rh_2(PhNOCCH_3)_4$.

Mass Spectrographic Analysis of Reaction Products. The parent ion mass for each reaction product was determined with an LC–MS system whose construction is described in the literature.[11] Each reaction product was analyzed from a 1 μg/mL sample in methanol. This sample was injected into the mass spectrometer via a high-pressure loop injector and chromatographic pump. The flow rate of the mobile phase (methanol) varied betwen 0.5 and 4 mL/min. Samples were introduced into the vaporizer by means of a stainless steel capillary tube that was heated to produce a thermal spray. Negative parent ions were produced by using a soft ionization technique operating in the negative-ion mode using an external ionization source. The ions were detected with a quadrupole mass filter coupled with an electron multiplier that had a 2000-amu range. All data were stored with a Finnigan-INCOS 2300 data system.

^{13}C NMR Spectroscopy. The ^{13}C NMR spectra were obtained with a Varian Model XL-100 spectrometer equipped with a Nicolet 1180 data system. All samples were dissolved in $CDCl_3$. $^{13}CDCl_3$ was used as an internal reference for the ^{13}C NMR spectra.

X-ray Data Collection for $Rh_2(PhNOCCH_2)_4Me_2SO$ ($7(Me_2SO)$). A large deep aquamarine block of approximate dimensions 0.60 × 0.30 × 0.30 mm was mounted on a glass fiber in a random orientation on an Enraf-Nonius CAD-4 automatic diffractometer. The radiation used was Mo Kα monochromatized by a dense graphite crystal assumed for all purposes to be 50% imperfect. Final cell constants, as well as other information pertinent to data collection and refinement, are listed in Table I. The Laue symmetry was determined to be 1, and from the systematic absences noted the space group was shown to be either *P*1 or *P*$\bar{1}$. Intensities were measured by using the θ–2θ scan technique, with the scan rate depending on the net count obtained in rapid prescans of each reflection. Two standard reflections were monitored periodically during the course of the data collection as a check of crystal stability and electronic reliability. These initially showed extremely rapid decay, such that the experiment had to be terminated and the data discarded. However, it was found that the sample at this point was still crystalline and in fact exhibited a higher quality than before (as measured by the peak widths at half-height). A new data collection was initiated on the same crystal, and the two new standard reflections that were chosen showed no sign of decay during the entire course of the experiment. In reduction of the data, Lorentz and polarization factors were applied. However, no correction for absorption was made due to the low absorption coefficient.

The structure was solved by the Patterson method, which revealed the positions of the two Rh atoms in the asymmetric unit, which comprised

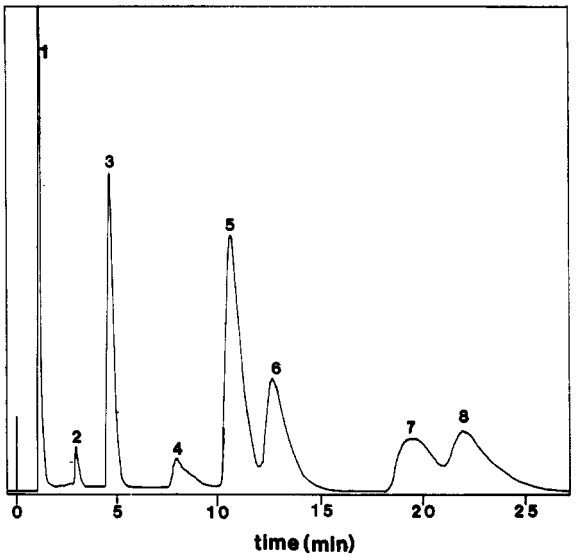

Figure 2. Chromatogram showing the separation of the various isomers and products from the exchange reaction: (**1**) $Rh_2(O_2CCH_3)_4$; (**2**) $Rh_2(O_2CCH_3)_3(PhNOCCH_3)$; (**3** and **4**) $Rh_2(O_2CCH_3)_2(PhNOCCH_3)_2$; (**5** and **6**) $Rh_2(O_2CCH_3)(PhNOCCH_3)_3$; (**7** and **8**) $Rh_2(PhNOCCH_3)_4$.

Table I. Data Collection and Processing Parameters of Compounds $7(Me_2SO)$ and $8(Me_2SO)_2$

	$7(Me_2SO)$	$8(Me_2SO)_2$
space group	$P\bar{1}$, triclinic	$Pna2_1$, orthorhombic
cell constants		
a, Å	8.333 (8)	15.780 (4)
b, Å	13.069 (4)	11.170 (5)
c, Å	17.641 (7)	21.212 (4)
α, deg	101.36 (2)	
β, deg	95.48 (6)	
γ, deg	104.00 (5)	
V, Å^3	1807	3739
mol formula	$Rh_2SO_5N_4C_{34}H_{38}$	$Rh_2S_2O_6N_4C_{36}H_{44}$
fw	820.6	898.7
formula units per cell (*Z*)	2	4
density (ρ), g cm^{-3}	1.51	1.60
abs coeff (μ), cm^{-1}	9.96	10.24
radiation (Mo Kα, λ), Å	0.71073	0.71073
collection range, deg	$4 \le 2\theta \le 35$	$4 \le 2\theta \le 47$
scan width (Δθ), deg	1.05 + 0.35 tan θ	1.10 + 0.35 tan θ
max scan time, s	150	150
scan speed range, deg min^{-1}	0.6–5.0	0.7–5.0
total data collected	2148	3151
indep data, $I > 3\sigma(I)$	1817	2239
total variables	419	450
$R = \sum\|\|F_o\| - \|F_c\|\|/\sum\|F_o\|$	0.038	0.027
$R_w = [\sum w(\|F_o\| - \|F_c\|)^2/\sum w\|F_o\|^2]^{1/2}$	0.040	0.031
weights (*w*)	σ_F^{-2}	σ_F^{-2}

one full molecule in the centrosymmetric space group $P\bar{1}$. The remaining non-hydrogen atoms were located in subsequent difference Fourier syntheses. The usual sequence of isotropic and anisotropic refinement was followed, after which all hydrogens were entered in ideally calculated positions. The methyl hydrogens of the acetamides were positioned so as to stagger the *N*-phenyl bonds. None of the hydrogen parameters were varied in the final cycles of full-matrix least squares. Hydrogen isotropic temperature factors were estimated on the basis of the thermal motion of the associated carbons. At this point, a small amount of residual electron density was found. This appeared to be a remnant of a solvent molecule of crystallization, which apparently did not totally evacuate during the initial decay period. This electron density was refined as an oxygen atom with an occupancy factor of 40%, based on the equivalent isotropic temperature factors of the other atoms in the refinement. After all shift/esd ratios were less than 0.1, convergence was reached at the agreement factors listed in Table I. No unusually high correlations were noted between any of the variables in the last cycle of least-squares refinement, and the final difference density map showed no peaks greater than 0.20 e/Å^3. All calculations were made by using Molecular Structure Corp.'s TEXRAY 230 modifications of the SDP-PLUS series of programs.

X-ray Data Collection for $Rh_2(PhNOCCH_3)_4(Me_2SO)_2$ (8(Me_2SO)$_2$). A large blood red tabular crystal of approximate dimensions 0.70 × 0.40 × 0.15 mm was mounted on a glass fiber in a random orientation on an Enraf-Nonius CAD-4 automatic diffractometer. The radiation used was Mo Kα monochromatized by a dense graphite crystal assumed for all purposes to be 50% imperfect. Final cell constants, as well as other information pertinent to data collection and refinement, are listed in Table I. The Laue symmetry was determined to be *mmm*, and from the noted systematic absences the space group was shown to be either *Pnma* or $Pn2_1a$. Intensities were measured by using the θ–2θ scan technique, with the scan rate depending on the net count obtained in rapid prescans of each reflection. As a check of crystal stability and electronic reliability two standard reflections were monitored periodically during the course of the data collection, and these did not vary significantly. Lorentz and polarization factors were applied in reducing the data. However, no correction for absorption was made due to the low absorption coefficient.

The structure was solved by MULTAN,[12] which revealed the positions of the two Rh and two S atoms in the asymmetric unit, which comprised one full molecule in the noncentrosymmetric space group $Pna2_1$. The data were collected as $Pn2_1a$ and later converted to the conventional setting. The remaining non-hydrogen atoms were located in subsequent difference Fourier syntheses. The usual sequence of isotropic and anisotropic refinement was followed, after which all hydrogens were entered in ideally calculated positions, with the acetamide methyl groups positioned so as to stagger the *N*-phenyl bonds. None of the hydrogen parameters were varied in the final cycles of full-matrix least squares. Hydrogen isotropic temperature factors were estimated on the basis of the thermal motion of the associated carbons. Convergence was reached at the agreement factors listed in Table I after all shift/esd ratios were less than 0.6. No unusually high correlations were noted between any of the variables in the last cycle of least-squares refinement, and the final difference density map showed no peaks located near Rh that were greater than 0.80 e/Å^3. All calculations were made by using Molecular Structure Corp.'s TEXRAY 230 modifications of the SDP-PLUS series of programs. No attempt was made to refine the enantiomeric set of coordinates in this polar space group.

Results and Discussion

A chromatogram showing the products formed in the reaction of $Rh_2(O_2CCH_3)_4$ and *N*-phenylacetamide is shown in Figure 2. Table II lists the molecular weights and corresponding formulas for the compound in each of the HPLC bands.

The isomer distribution among the different substitution products from the reaction with *N*-phenylacetamide is different from that observed for acetamide. The exchange reaction involving $Rh_2(O_2CCH_3)_4$ and acetamide results in six reaction products[9,10] instead of seven as in the present case. The distribution of isomers for acetamide complexes with n = 0, 1, 2, and 3 was 1:1:3:1, whereas for complexes of *N*-phenylacetamide with the same n value the isomer distribution was 2:2:2:1. Also, the rate of acetate substitution by acetamide is much faster than acetate substitution by *N*-phenylacetamide.

The mechanism proposed for equatorial ligand exchange of dirhodium(II) complexes involves the initial formation of an axial adduct by the incoming ligand followed by a substitution of the bridging ligand.[13] This process involves both bond-forming and bond-breaking steps and the exchange of a proton from the entering ligand to the leaving ion. The sequence and geometric location of the bond-breakage and bond-formation processes are reflected in geometric isomer products whenever the entering ligand includes a hetero donor atom. The isomer distribution for the acetamide reaction[13] can be explained by simply imposing the restriction that two Rh–N bonds are never formed trans to each other on the same rhodium ion. This suggests that the addition of each successive acetamide has a directing influence on the next substitution process.

Table II. LC–MS Results for the Collected Bands in CH_3OH[a]

formula	parent ion mass, amu	compd (HPLC band)
$Rh_2(O_2CCH_3)_4$	441.8	**1**
$Rh_2(O_2CCH_3)_3(PhNOCCH_3)$	516.8	**2**
$Rh_2(O_2CCH_3)_2(PhNOCCH_3)_2$	591.9	**3**
	591.4	**4**
$Rh_2(O_2CCH_3)(PhNOCCH_3)_3$	667.0	**5**
	667.3	**6**
$Rh_2(PhNOCCH_3)_4$	742.8	**7**
	743.1	**8**

[a] Operating in the negative-ion mode; estimated error ±1.0 amu.

The nature of the Rh–ligand axial bond should also influence which geometric isomers are formed, i.e. those containing a Rh–N or those containing a Rh–O axial bond. For this reason the substitution reaction should be sensitive to any steric factors that are related to axial bond formation. The slow rate of substitution and the different geometric isomer distributions observed for *N*-phenylacetamide and acetamide suggest that this is the case. The *N*-phenyl group on the amide nitrogen inhibits axial bond formation through the amide nitrogen. Also, once substitution has occurred, the axial site of the rhodium ion with the least number of Rh–N bonds would be the least sterically hindered with respect to adduct formation by the entering ligand. Thus, both electronic and steric factors appear to be involved in determining which geometric isomers are formed for the different substitution products. Unfortunately, a detailed mechanistic study of the overall exchange process is not feasible with *N*-phenylacetamide. This is because of the complexity of this multireaction system and the decomposition processes that result from the extreme reaction conditions (i.e. high temperature and long time needed to accomplish the substitution). However, this system does provide two geometric isomers of the bis-, tris-, and tetrakis-substituted dirhodium complexes, which can be used in a study of isomer effects on the chemistry and electrochemistry of these complexes.

Molecular Structures: Dimethyl Sulfoxide Adducts of Compounds 7 and 8. An identification of the various $Rh_2(O_2CCH_3)_n(PhNOCCH_3)_{4-n}$ isomers is important for a mechanistic understanding of the equatorial-ligand-exchange reaction. Molecular structures of Me_2SO adducts of the $Rh_2(PhNOCCH_3)_4$ isomers can also be instrumental in helping to identify isomers of other $Rh_2(O_2CCH_3)_n(PhNOCCH_3)_{4-n}$ complexes.

Labeled ORTEP diagrams of the Me_2SO adducts of compounds **7** and **8** are shown in parts a and b, respectively, of Figure 3. Selected bond lengths and bond angles are listed in Table III, and the positional parameters for each complex are given in Table IV. As seen in Figure 3b each rhodium atom of compound **8**(Me_2SO)$_2$ is bonded to two nitrogen and two oxygen donor atoms from the ligand in a cis arrangement. This arrangement is the same as that shown in structure IVa of Figure 1. A similar structure is also observed for the bis(dimethyl sulfoxide) adduct of $Rh_2(HNOCCH_3)_4$. Compound **7**(Me_2SO) differs from compound **8**(Me_2SO)$_2$ in that one rhodium atom is bonded to three nitrogens while the other rhodium is bonded to one nitrogen (structure IVc, Figure 1). Compound **8**(Me_2SO)$_2$ is capable of binding dimethyl sulfoxide at each axial site. In contrast, compound **7**(Me_2SO) forms only a mono(dimetyl sulfoxide) adduct. The steric effect of three *N*-phenyl groups around one of the rhodiums of compound **7**(Me_2SO) inhibits the formation of a bis(dimethyl sulfoxide) adduct. This steric effect of three *N*-phenyl groups around one rhodium atom is also reflected in the N–Rh–Rh–O torsional angle. In compound **7**(Me_2SO) this angle is 13.3° while in compound **8**(Me_2SO)$_2$ and in $Rh_2(HNOCCH_3)_4$ it is <4°.

Table III. Selected Bond Lengths and Angles of Compounds $7(Me_2SO)$ and $8(Me_2SO)_2$[a,b]

(a) Selected Bond Lengths (Å)

bond	$7(Me_2SO)$	$8(Me_2SO)_2$
Rh–Rh	2.397 (1)	2.448 (1)
Rh1–S1		2.606 (2)
Rh2–S2	2.395 (1)	2.566 (2)
Rh1–O	2.065 (3)	2.041 (4)
Rh1–N	2.027 (4)	2.056 (5)
Rh2–O	2.044 (3)	2.035 (4)
Rh2–N	2.047 (4)	2.061 (5)
S1–O		1.472 (5)
S1–C		1.782 (8)
S2–O	1.468 (3)	1.469 (4)
S2–C	1.768 (5)	1.761 (7)
C–O	1.279 (5)	1.276 (10)
C–N	1.305 (6)	1.292 (8)
N–C(Ph)	1.406 (6)	1.429 (8)
C–CH_3	1.520 (7)	1.514 (8)

(b) Selected Bond Angles (deg)

	$7(Me_2SO)$		
Rh1–Rh2–S	174.14 (4)	N1–Rh1–N2	90.0 (1)
Rh–Rh–O	88.0 (1)	N1–Rh1–N4	173.4 (2)
Rh–Rh–N	86.9 (2)	N1–Rh1–O3	88.9 (1)
Rh2–S–O5	122.9 (2)	O1–Rh2–O2	93.7 (1)
O–C–N	122.2 (6)	O1–Rh2–O4	175.8 (1)
S–Rh–O	90.4 (1)	O1–Rh2–N3	87.6 (1)
S–Rh2–N3	98.8 (2)	N–Rh–Rh–O	13.1[c]
	$8(Me_2SO)_2$		
Rh–Rh–S	173.35 (5)	S–Rh–O	85.6 (1)
Rh–Rh–O	89.9 (1)	S–Rh–N	99.4 (2)
Rh–Rh–N	85.8 (2)	O–Rh–O	88.2 (2)
Rh–S–O	127.4 (2)	N–Rh–N	93.7 (2)
O–C–N	123.7 (6)	N–Rh–Rh–O	3.48[c]

[a] Numbers in parentheses are estimated standard deviations in the least significant digits. [b] All angles are averages except when atoms are numbered. [c] Average torsional angle about Rh–Rh bond.

The effect of the number of bound axial dimethyl sulfoxide ligands on the Rh–Rh bond length is dramatic. The Rh–Rh bond distances of the bis(dimethyl sulfoxide) adducts of compound **8** and of $Rh_2(HNOCCH_3)_4$ are 2.448 and 2.452 Å, respectively. This is a difference of only 0.004 Å. The Rh–Rh distance of the mono(dimethyl sulfoxide) adduct of compound **7** (2.397 Å) is shorter by 0.051 Å than that of the bis(dimethyl sulfoxide) adduct of compound **8**. Furthermore, it can be seen that the Rh–S axial bond distance in the mono(dimethyl sulfoxide) adduct of compound **7** (2.395 Å) is much shorter than the Rh–S distance in the bis(dimethyl sulfoxide) adduct of compound **8**. Comparison of the average Rh–S bond distance in the Me_2SO bisadducts of compound **8** (2.586 Å) and $Rh_2(HNOCCH_3)_4$ (2.414 Å) shows that although their Rh–Rh distances are similar, the Rh–S distance in the latter complex is much shorter. The Rh–S bond distances given in Table III are directly related to the magnitudes of the formation constants between dimethyl sulfoxide and the particular dirhodium complex, but the Rh–Rh bond distance appears to depend on a number of factors.[14] This is discussed in following sections of this paper.

^{13}C NMR Spectra of Compounds 2–8. The ^{13}C NMR spectra were recorded in order to elucidate possible structural differences of the $Rh_2(O_2CCH_3)(PhNOCCH_3)_3$ isomers (compounds **5** and **6**). Indeed, the carbonyl region of the ^{13}C NMR spectra of compounds **7** and **8** does reveal structural differences. Compound **7** exhibits the predicted three amide carbonyl resonances at 180.0, 180.3, and 180.9 ppm. Compound **8** had only one resonance for the bridging carbonyls at 180.1 ppm. This is consistent for a symmetrical arrangement of the bridging ligands.

The ^{13}C NMR spectrum of compound **5** shows three nonequivalent amide carbonyl carbon atoms at resonances of 179.9, 180.4, and 181.5 ppm. The acetate carbonyl appears at 187.2 ppm. This suggests that compound **5** has structure IIIa (Figure 1).

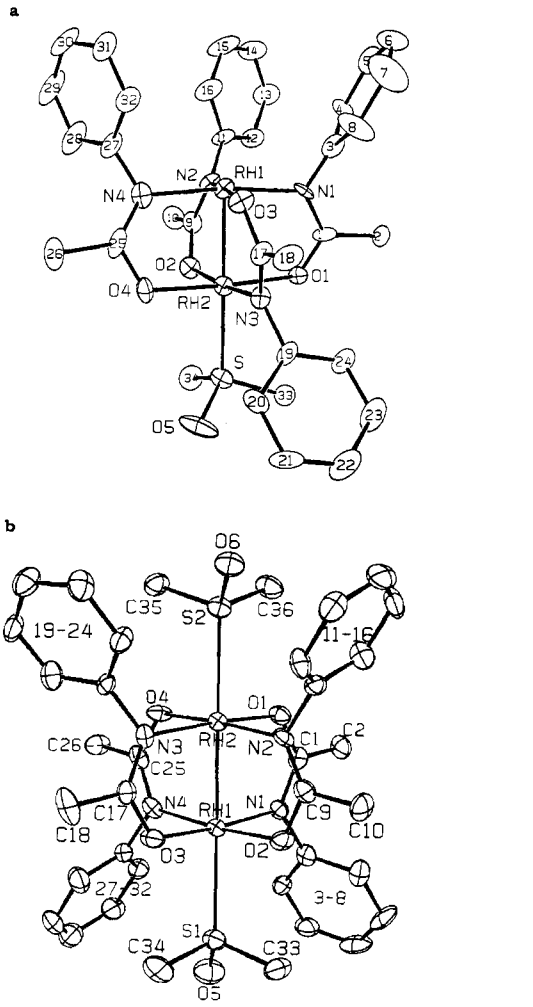

Figure 3. Labeled ORTEP diagrams of the molecular structures of (a) $Rh_2(PhNOCCH_3)_4Me_2SO$ ($7(Me_2SO)$) and (b) $Rh_2(PhNOCCH_3)_4(Me_2SO)_2$ ($8(Me_2SO)_2$). The thermal ellipsoids are represented as 35% equiprobability envelopes.

Compound **6** shows two types of amide carbonyls in its ^{13}C NMR spectrum. These occur at 180.3 and 181.0 ppm. The acetate carbonyl appears at 187.6 ppm. Compound **6** could have either structure IIb or IIIc, but the two structures cannot be distinguished from the available data. The structures of compounds **3** and **4** also cannot be determined since they both have nearly identical ^{13}C NMR spectra that are consistent with structures IIa–d.

Electrochemistry and Dimethyl Sulfoxide Binding Constants of Compounds 2–8. Dirhodium complexes of the type $Rh_2(O_2CCH_3)_n(L)_{4-n}$ (where L is a bidentate ligand having N–O, N–S, or N–N donor atoms) may undergo the metal-centered oxidations shown by reactions 1 and 2. The exact potentials and

$$Rh^{II}Rh^{II} \rightleftarrows Rh^{II}Rh^{III} + e^- \quad (1)$$

$$Rh^{II}Rh^{III} \rightleftarrows Rh^{III}Rh^{III} + e^- \quad (2)$$

nature of these reactions will depend upon the value of n and the electron-donating ability of the individual ligand L.

The electrochemistry of compound **8** has been characterized in detail.[7,8] This compound undergoes reactions 1 and 2 at $E_{1/2}$ = 0.55 and 1.65 V vs. SCE in methylene chloride, and its ESR and electronic absorption spectra support metal-centered oxidations. Compound **7** also undergoes two reversible oxidations at $E_{1/2}$ = 0.60 and 1.70 V in the same solvent.[7] The frozen-glass ESR spectrum of the $Rh^{II}Rh^{III}$ species obtained from oxidation of compound **7** is identical with that obtained after oxidation of compound **8**.[8] This is not surprising since the ESR spectra of all $[Rh_2(O_2CCH_3)_n(HNOCCH_3)_{4-n}]^+$ complexes are virtually identical and have the same $g_\perp$, $g_\parallel$, and $A_\parallel$ values in CH_3CN and

Table IV. Positional Parameters and Their Estimated Standard Deviations[a]

atom	x	y	z	B, Å²	atom	x	y	z	B, Å²
				(a) 7(Me_2SO)					
Rh1	0.1446 (1)	0.18401 (6)	0.27569 (5)	3.44 (2)	C32	0.258 (1)	−0.0427 (8)	0.2702 (6)	4.6 (3)
Rh2	0.1051 (1)	0.20203 (6)	0.17710 (5)	3.42 (2)	C33	0.004 (2)	0.4986 (9)	0.1221 (7)	6.6 (4)
S	0.0354 (4)	0.3727 (2)	0.0782 (2)	4.52 (8)	C34	−0.171 (1)	0.3072 (9)	0.0299 (7)	6.3 (4)
O1	0.0445 (7)	0.3928 (5)	0.2606 (3)	3.2 (2)	O6	0.319 (2)	0.216 (1)	0.981 (1)	6.1 (5)
O2	−0.1350 (8)	0.1841 (5)	0.1484 (4)	4.6 (2)	H2A	0.0228	0.5456	0.3582	6*
O3	0.3997 (7)	0.2480 (5)	0.2849 (4)	4.2 (2)	H2B	−0.0192	0.4686	0.4259	6*
O4	0.1660 (8)	0.1650 (5)	0.0997 (4)	4.6 (2)	H2C	0.1832	0.5354	0.4224	6*
O5	0.1363 (9)	0.3903 (7)	0.0159 (4)	9.4 (3)	H4	−0.0441	0.2680	0.4591	6*
N1	0.1354 (9)	0.3169 (6)	0.3529 (4)	3.0 (2)	H5	0.0298	0.2661	0.5849	6*
N2	−0.1101 (9)	0.1259 (6)	0.2604 (5)	3.8 (2)	H6	0.3029	0.3100	0.6397	6*
N3	0.3500 (9)	0.3680 (6)	0.2124 (4)	3.6 (2)	H7	0.5079	0.3704	0.5651	6*
N4	0.1558 (9)	0.0605 (6)	0.1884 (5)	4.4 (2)	H8	0.4247	0.3688	0.4347	6*
C1	0.083 (1)	0.3957 (7)	0.3309 (5)	3.5 (3)	H10A	−0.4259	0.0858	0.1211	6*
C2	0.066 (1)	0.4940 (8)	0.3890 (6)	4.7 (3)	H10B	−0.3930	−0.0129	0.1671	6*
C3	0.182 (1)	0.3205 (7)	0.4275 (6)	4.7 (3)	H10C	−0.4474	0.0965	0.2179	6*
C4	0.073 (2)	0.2897 (9)	0.4786 (6)	6.7 (4)	H12	−0.3522	0.1759	0.3330	6*
C5	0.115 (2)	0.2875 (9)	0.5543 (8)	7.6 (4)	H13	−0.4484	0.1227	0.4435	6*
C6	0.273 (2)	0.314 (1)	0.5871 (7)	8.6 (4)	H14	−0.3393	0.0031	0.4970	6*
C7	0.392 (2)	0.348 (2)	0.5439 (9)	12.8 (7)	H15	−0.1354	−0.0650	0.4436	6*
C8	0.339 (2)	0.348 (1)	0.4651 (7)	10.0 (5)	H16	−0.0376	−0.0116	0.3358	6*
C9	−0.199 (1)	0.1303 (8)	0.1970 (6)	4.1 (3)	H18A	0.6882	0.3437	0.3171	6*
C10	−0.380 (1)	0.0704 (9)	0.1739 (6)	5.5 (4)	H18B	0.6953	0.3873	0.2317	6*
C11	−0.182 (1)	0.0878 (7)	0.3240 (6)	4.0 (3)	H18C	0.6538	0.4668	0.3130	6*
C12	−0.306 (1)	0.1271 (8)	0.3558 (6)	5.0 (3)	H20	0.5004	0.4007	0.0901	6*
C13	−0.364 (1)	0.0949 (9)	0.4207 (7)	6.8 (4)	H21	0.6123	0.5686	0.0582	6*
C14	−0.299 (2)	0.0250 (9)	0.4523 (7)	7.5 (4)	H22	0.5739	0.7249	0.1323	6*
C15	−0.180 (2)	−0.0151 (9)	0.4213 (8)	8.6 (4)	H23	0.4557	0.7229	0.2450	6*
C16	−0.122 (1)	0.0168 (8)	0.3576 (7)	6.5 (4)	H24	0.3498	0.5593	0.2778	6*
C17	0.450 (1)	0.3327 (7)	0.2572 (6)	3.9 (3)	H26A	0.2078	0.0230	0.0019	6*
C18	0.637 (1)	0.3869 (8)	0.2817 (6)	4.9 (3)	H26B	0.3186	−0.0231	0.0685	6*
C19	0.418 (1)	0.4657 (7)	0.1883 (6)	3.8 (3)	H26C	0.1078	−0.0805	0.0411	6*
C20	0.493 (1)	0.4666 (9)	0.1218 (6)	5.6 (3)	H28	−0.0658	−0.1304	0.1313	6*
C21	0.556 (1)	0.5661 (9)	0.1025 (6)	6.7 (4)	H29	−0.0824	−0.2877	0.1746	6*
C22	0.536 (2)	0.6582 (9)	0.1475 (8)	7.8 (4)	H30	0.1034	−0.2920	0.2798	6*
C23	0.464 (1)	0.6569 (9)	0.2132 (8)	6.9 (4)	H31	0.3211	−0.1348	0.3405	6*
C24	0.403 (1)	0.5601 (8)	0.2324 (6)	5.0 (3)	H32	0.3461	0.0204	0.2941	6*
C25	0.169 (1)	0.0746 (7)	0.1191 (7)	4.8 (3)	H33A	0.1167	0.5494	0.1542	6*
C26	0.203 (1)	−0.0081 (9)	0.0522 (7)	6.7 (4)	H33B	−0.0383	0.5339	0.0783	6*
C27	0.146 (1)	−0.0418 (8)	0.2078 (7)	5.1 (3)	H33C	−0.0863	0.4860	0.1594	6*
C28	0.014 (1)	−0.1328 (9)	0.1728 (8)	7.6 (4)	H34A	−0.1755	0.2286	−0.0002	6*
C29	0.004 (2)	−0.2244 (9)	0.1997 (9)	8.8 (5)	H34B	−0.2530	0.3032	0.0714	6*
C30	0.114 (2)	−0.2274 (8)	0.2614 (8)	8.6 (4)	H34C	−0.2050	0.3512	−0.0096	6*
C31	0.244 (1)	−0.1339 (8)	0.2973 (7)	6.6 (4)					
				(b) 8(Me_2SO)$_2$					
Rh1	0.88041 (4)	0.81661 (6)	0.301	2.04 (1)	C17	0.9826 (5)	0.7201 (7)	0.4018 (5)	2.4 (2)
Rh2	0.85084 (4)	0.90641 (6)	0.40415 (5)	1.97 (1)	C18	1.0477 (6)	0.6314 (9)	0.4278 (6)	4.4 (3)
S1	0.9352 (2)	0.7246 (2)	0.1959 (1)	3.19 (6)	C19	0.9417 (5)	0.7668 (8)	0.5062 (4)	2.2 (2)
S2	0.8009 (2)	0.9981 (2)	0.5087 (1)	2.81 (5)	C20	0.9039 (6)	0.6639 (8)	0.5315 (5)	3.5 (2)
O1	0.7600 (4)	1.0084 (6)	0.3633 (3)	2.6 (1)	C21	0.9076 (7)	0.6401 (9)	0.5939 (5)	3.7 (2)
O2	0.9650 (4)	0.9506 (6)	0.2836 (3)	2.8 (1)	C22	0.9451 (7)	0.719 (1)	0.6347 (5)	4.0 (3)
O3	0.9762 (4)	0.7229 (6)	0.3433 (3)	2.9 (1)	C23	0.9800 (7)	0.8219 (9)	0.6130 (5)	3.9 (3)
O4	0.7601 (4)	0.7788 (5)	0.4197 (3)	2.7 (1)	C24	0.9795 (6)	0.8444 (8)	0.5475 (5)	3.1 (2)
O5	0.8870 (5)	0.6647 (7)	0.1456 (4)	5.1 (2)	C25	0.7520 (6)	0.6935 (8)	0.3802 (5)	2.7 (2)
O6	0.8544 (4)	1.0626 (6)	0.5540 (3)	3.7 (2)	C26	0.6881 (6)	0.5995 (9)	0.3999 (6)	3.6 (2)
N1	0.7879 (5)	0.9268 (6)	0.2678 (3)	2.2 (2)	C27	0.7872 (6)	0.5793 (7)	0.2909 (4)	2.7 (2)
N2	0.9397 (4)	1.0332 (6)	0.3804 (3)	2.2 (2)	C28	0.8470 (6)	0.4880 (9)	0.2972 (6)	4.4 (2)
N3	0.9397 (5)	0.7888 (6)	0.4400 (4)	2.5 (2)	C29	0.8379 (9)	0.3860 (9)	0.2587 (5)	5.4 (3)
N4	0.7955 (5)	0.6852 (7)	0.3294 (4)	2.7 (2)	C30	0.7745 (8)	0.3758 (9)	0.2170 (5)	4.9 (3)
C1	0.7477 (5)	1.0021 (7)	0.3048 (5)	2.5 (2)	C31	0.7177 (7)	0.4666 (9)	0.2113 (5)	4.0 (3)
C2	0.6803 (6)	1.0847 (9)	0.2803 (5)	3.4 (2)	C32	0.7233 (7)	0.5664 (8)	0.2481 (5)	3.2 (2)
C3	0.7801 (5)	0.9368 (8)	0.2015 (5)	2.6 (2)	C33	0.9991 (7)	0.897 (1)	0.1586 (5)	3.9 (2)
C4	0.8157 (6)	1.0330 (9)	0.1679 (5)	3.4 (2)	C34	1.0190 (7)	0.626 (1)	0.2157 (6)	5.4 (3)
C5	0.8091 (7)	1.038 (1)	0.1021 (5)	4.6 (3)	C35	0.7435 (6)	0.8886 (9)	0.5503 (5)	3.5 (2)
C6	0.7709 (7)	0.949 (1)	0.0691 (5)	4.7 (3)	C36	0.7136 (6)	1.0916 (9)	0.4926 (5)	3.9 (2)
C7	0.7362 (7)	0.8567 (9)	0.1011 (5)	4.1 (3)	H2A	0.6549	1.1362	0.3142	5*
C8	0.7402 (6)	0.8489 (8)	0.1655 (4)	2.8 (2)	H2B	0.7027	1.1389	0.2459	5*
C9	0.9762 (6)	1.0342 (8)	0.3272 (5)	2.7 (2)	H2C	0.6315	1.0364	0.2607	5*
C10	1.0351 (6)	1.1324 (9)	0.3053 (6)	3.4 (2)	H4	0.8453	1.0966	0.1915	5*
C11	0.9525 (6)	1.1336 (8)	0.4212 (4)	2.5 (2)	H5	0.8304	1.1058	0.0789	5*
C12	0.8976 (7)	1.2304 (9)	0.4186 (5)	3.9 (2)	H6	0.7671	0.9499	0.0225	5*
C13	0.9086 (8)	1.3270 (9)	0.4585 (6)	5.2 (3)	H7	0.7112	0.7927	0.0773	5*
C14	0.9768 (8)	1.3281 (9)	0.5008 (5)	4.7 (3)	H8	0.7139	0.7799	0.1870	5*
C15	1.0307 (7)	1.233 (1)	0.5025 (5)	3.8 (2)	H10A	1.0562	1.1144	0.2613	5*
C16	1.0199 (6)	1.1358 (8)	0.4621 (5)	3.2 (2)	H10B	1.0043	1.2117	0.3038	5*

Table IV (Continued)

atom	x	y	z	B, Å²	atom	x	y	z	B, Å²
H10C	1.0847	1.1400	0.3340	5*	H28	0.8945	0.4966	0.3272	5*
H12	0.8494	1.2315	0.3893	5*	H29	0.8804	0.3210	0.2626	5*
H13	0.8697	1.3951	0.4562	5*	H30	0.7697	0.3047	0.1914	5*
H14	0.9841	1.3952	0.5269	5*	H31	0.6744	0.4606	0.1786	5*
H15	1.0765	1.2307	0.5306	5*	H32	0.6787	0.6271	0.2437	5*
H16	1.0603	1.0688	0.4634	5*	H33A	0.9630	0.9053	0.1442	5*
H18A	1.0744	0.5832	0.3927	5*	H33B	1.0413	0.8704	0.1910	5*
H18B	1.0933	0.6716	0.4524	5*	H33C	1.0316	0.8036	0.1230	5*
H18C	1.0186	0.5708	0.4573	5*	H34A	0.9986	0.5518	0.2376	5*
H20	0.8740	0.6054	0.5012	5*	H34B	1.0523	0.5997	0.1768	5*
H21	0.8816	0.5654	0.6101	5*	H34C	1.0620	0.6665	0.2449	5*
H22	0.9517	0.6976	0.6803	5*	H35A	0.7816	0.8205	0.5638	5*
H23	1.0014	0.8851	0.6424	5*	H35B	0.7145	0.9222	0.5877	5*
H24	1.0057	0.9160	0.5316	5*	H35C	0.6979	0.8514	0.5215	5*
H26A	0.6612	0.6235	0.4433	5*	H36A	0.7316	1.1644	0.4688	5*
H26B	0.6418	0.5901	0.3697	5*	H36B	0.6695	1.0474	0.4673	5*
H26C	0.7159	0.5189	0.4082	5*	H36C	0.6862	1.1182	0.5335	5*

[a] Starred values are for atoms refined isotropically. Anisotropically refined atoms are given in the form of the isotropic equivalent thermal parameter defined as $^4/_3[a^2B_{11} + b^2B_{22} + c^2B_{33} + ab(\cos\gamma)B_{12} + ac(\cos\beta)B_{13} + bc(\cos\alpha)B_{23}]$.

Table V. Comparison of Electrochemical and Spectroscopic Properties of $Rh_2(O_2CCH_3)_n(PhNOCCH_3)_{4-n}$ in CH_2Cl_2 and Me_2SO

compd	band[a]	$E_{1/2}$, V			λ_{max}, nm[b]		log	log	assigned
		CH_2Cl_2	Me_2SO	Δ[d]	Me_2Cl_2	Me_2SO	K_1[c]	K_2[c]	structure[h]
$Rh_2(O_2CCH_3)_4$	1	~1.3[e]	1.0	0.3		503	1.04[g]	−0.22[g]	
$Rh_2(O_2CCH_3)_3(PhNOCCH_3)$	2	1.13	0.88	0.22	655	502	4.3	1.23	I
$Rh_2(O_2CCH_3)_2(PhNOCCH_3)_2$	3	0.97	0.73	0.24	652	509	3.0	0.90	*i*
	4	0.95	0.76	0.19	650	518	3.4	0.41	*i*
$Rh_2(O_2CCH_3)(PhNOCCH_3)_3$	5	0.76	0.55	0.21	651	517	2.2	0.45	IIIa
	6	0.76	0.51	0.25	667	546	2.4	0.04	IIIb
$Rh_2(PhNOCCH_3)_4$	7	0.60	0.41	0.19	700	585	3.1	*f*	IVc
	8	0.55	0.40	0.15	668	513	2.0	0.08	IVa

[a] Band numbers based on the sequence of LC separation. [b] Wavelength of the peak ($\epsilon \simeq 10^2$) in the visible region; neat solvent. [c] K_1 and K_2 are formation constants of the Me_2SO mono- and bisadducts, respectively, measured in CH_2Cl_2. [d] $E_{1/2}(CH_2Cl_2) - E_{1/2}(Me_2SO)$. [e] Estimation based on $E_{1/2}$ for $Rh_2(O_2CC_2H_5)$ in CH_2Cl_2, 1.2 V ($Rh_2(O_2CCH_3)_4$ is poorly soluble in CH_2Cl_2). [f] Even in neat Me_2SO no bisadduct appears to form. [g] Taken from ref 9. [h] See Figure 1. [i] Structure not assigned.

Me_2SO.[10] This is true in spite of the fact that each complex has a unique equatorial environment due to the different numbers of bridging acetamidate ligands.

Compounds **5** and **6** also undergo two reversible oxidations. The potentials for reaction 1 are identical (0.76 V) for these complexes in methylene chloride. The second oxidations of both compounds occur close to the solvent limit, and both are at $E_{1/2} \approx 1.75$ V. Compounds **2–4** show only one reversible oxidation within the solvent limit. This is similar to the electrochemistry of the $Rh_2(O_2CCH_3)_n(HNOCCH_3)_{4-n}$ complexes.[9,10] Also, the potentials for reactions 1 and 2 shift to more negative values as the number of bridging acetamidate ligands in these complexes increases. The potentials for reactions 1 are relevant to the main theme of this study and are listed in Table V.

Half-wave potentials for $Rh_2(O_2CCH_3)_n(PhNOCCH_3)_{4-n}$ oxidation in methylene chloride (reaction 1) range from 1.13 V for $n = 3$ to 0.55 V for $n = 0$ and the potential of each complex changes by 160–200 mV for each integral change in the value of n. In contrast, half-wave potentials for any two isomers differ by at most 50 mV (compounds **7** and **8**) or do not differ at all (compounds **5** and **6**).

Axial Binding by Dimethyl Sulfoxide: Significance of Formation Constants. Dimethyl sulfoxide binds to the $Rh_2(O_2CCH_3)_n(HNOCCH_3)_{4-n}$ complexes via its sulfur atom.[14] The equilibrium constants (K_1 and K_2) can be measured by both electrochemical and spectroscopic techniques, and the stepwise Me_2SO binding reactions are given by eq 3 and 4. In the present investigation

$$Rh_2 + Me_2SO \overset{K_1}{\rightleftharpoons} Rh_2(Me_2SO) \quad (3)$$

$$Rh_2(Me_2SO) + Me_2SO \overset{K_2}{\rightleftharpoons} Rh_2(Me_2SO)_2 \quad (4)$$

K_1 and K_2 were measured by monitoring changes in the electronic absorption spectra with use of techniques described elsewhere.[14] These measured formation constants are listed in Table V.

Formation constants for reactions 3 and 4 were noted to increase with increasing number of bridging acetamidate ligands on $Rh_2(O_2CCH_3)_n(HNOCCH_3)_{4-n}$ ($4 - n = 0$ to 4),[14] and this trend was rationalized in terms of the increased "softness" of the rhodium atoms with increasing number of acetamidate bridging ligands. However, in contrast to the data in Table V the formation constants of $Rh_2(O_2CCH_3)_n(PhNOCCH_3)_{4-n}$ do not follow a well-defined trend. In fact, the Me_2SO formation constants for compounds having the formula $Rh_2(O_2CCH_3)_n(PhNOCCH_3)_{4-n}$ become smaller with increasing number of $[PhNOCCH_3]^-$ bridging ligands. This opposite trend is undoubtedly due to a steric effect of the *N*-phenyl groups, which crowd the axial site. In fact, a close inspection of the K_1 and K_2 values may be helpful in assigning structures of at least some of the isomers that could not be distinguished by ^{13}C NMR spectroscopy. This is because isomers having different numbers of *N*-phenyl groups on each rhodium atom must have a different magnitude of steric hindrance at each of the axial sites.

The log K_1 value for $Rh_2(O_2CCH_3)_3(PhNOCCH_3)$ binding of Me_2SO is 4.3 (see Table V). This formation constant is much higher than that for $Rh_2(O_2CCH_3)_4$ (1.04). While the trend is as expected,[14] the difference between the formation constants for complexes with $n = 4$ and $n = 3$ is extraordinarily large when compared to the log K_1 values for $Rh_2(O_2CCH_3)_3(HNOCCH_3)$ (1.34)[14] and $Rh_2(O_2CCH_3)_4$ (1.04). Arguments based on steric factors may suggest that the first dimethyl sulfoxide molecule binds to the rhodium atom that is not attached to an *N*-phenyl group. However, the extraordinary stability of this adduct cannot be explained in such a case. On the other hand, if the ligand addition reaction occurs at one of the rhodiums that is bound to the N atom, then it is not clear why a sterically hindered site should give added stability to the bond between a Me_2SO molecule and the dirhodium complex. In fact, as will be seen below, the presence of more than one *N*-phenyl group on a rhodium atom decreases the formation constants for binding Me_2SO at that axial site.

The question as to where the first Me_2SO molecule binds cannot be resolved. However, for a given set of isomers, higher K_1 values may be associated with a "$Rh_2(O_2CCH_3)_3(PhNOCCH_3)$-like" structure (i.e. a structure in which one axial site has more *N*-phenyl groups around it than the other). In contrast, the isomer having a considerably lower K_1 value may be assumed to have a "more even" distribution of N donor atoms around the two rhodium atoms of the dimer. From this line of reasoning, compounds **4**, **6**, and **7** may be candidates for "$Rh_2(O_2CCH_3)_3(PhNOCCH_3)$-like" structures. The crystal structure of compound **7**(Me_2SO) (Figure 3a) supports this argument.

On the basis of ^{13}C NMR, it was suggested that compound **6** may have structure IIIb or IIIc shown in Figure 1. Structure IIIc, which has one axial site crowded as in compound **7** (see Figure 3a), will not bind a second Me_2SO molecule. This argues against structure IIIc. Therefore, it is more likely that compound **6** has structure IIIb.

Assignment of compounds **3** and **4** is uncertain. On the basis of their log K_1 values compound **4** has structure IIa or IIb while compound **3** has structure IIc or IId. This is because the steric environment of IIa should be the same as that of IIb with one axial site more crowded than the other. In contrast, structures IIc and IId have equal steric hindrance at each axial site. Unfortunately, a further distinction between structures IIa and IIb or IIc and IId cannot be made since IIa, IIc, and IId are all capable of leading to the formation of structure IIIa. Similarly, IIIb can be formed from either structure IIb or IIc.

In summary, this study has shown that the substitution of phenyl for hydrogen on the acetamide nitrogen changes the isomer distribution among the products. This appears to be due to steric factors involved in axial bond formation of the entering ligand. Significant isomer effects are not observed in the redox potentials. A moderate effect is observed in the electronic absorption spectra of the higher substitution products, and this isomer effect is reflected quite strongly in the formation constants for Me_2SO addition. Thus, it appears that steric crowding around the axial site of the two rhodium ions is a dominant factor in determining differences in chemical and structural properties of the geometric isomers.

Acknowledgment. The support of the Robert A. Welch Foundation (K.M.K., Grant E-680; J.L.B., Grant E-918) is gratefully acknowledged. We also wish to acknowledge Dr. James Korp, University of Houston X-ray Crystallography Center, for performing the X-ray analysis.

Supplementary Material Available: Listings of anisotropic thermal parameters and root-mean-square amplitudes of thermal vibration and complete listings of bond lengths and angles (20 pages); listings of observed and calculated structure factors (22 pages). Ordering information is given on any current masthead page.

Contribution from the Departments of Chemistry, Texas A&M University, College Station, Texas 77843, Universidad de Santiago, Santiago, Chile, and Faculty of Sciences, Universidad de Chile, Santiago, Chile

Characterization of Tetra-, Penta-, and Hexacoordinated High-Spin Iron(II) Complexes with Neutral Monodentate Sulfur Donor Ligands. Crystal and Molecular Structure of $Fe(DMTU)_7(BF_4)_2$ (DMTU = *N*,*N*'-Dimethylthiourea)

J. P. Fackler,*† T. Moyer,†‡ J. A. Costamagna,*§ R. Latorre,‖ and J. Granifo‖⊥

Received June 12, 1986

New cationic high-spin iron(II) complexes with substituted thioureas and with perchlorate or tetrafluoroborate anions (X) were obtained: $[FeL_6]X_2$ (L = *N*-ethylthiourea, *N*,*N*'-di-*n*-propylthiourea); $[FeL_n](ClO_4)_2$ (L = *N*,*N*'-dimethylthiourea, *N*,*N*'-diethylthiourea; *n* = 4, 6); $[Fe(DMTU)_n](BF_4)_2$ (DMTU = *N*,*N*'-dimethylthiourea; *n* = 4, 5, 7). Tetrahedral ($[FeL_4]X_2$), octahedral ($[FeL_6]X_2$, $[Fe(DMTU)_6](BF_4)_2$·DMTU), and pentacoordinate ($[Fe(DMTU)_5](BF_4)_2$) structures have been identified by using electronic and Mössbauer spectroscopies and magnetic susceptibility measurements. For the last structure, a square-base-pyramidal symmetry around the iron atom is proposed. The DMTU complexes are the first examples in which a soft sulfur-binding monodentate ligand is found in binary iron complexes with three different arrangements. It was possible to evaluate the distortion in the tetrahedral complexes ($\Delta_T \sim 800$ cm^{-1}) and to correlate the isomer shift with the coordination number: tetracoordinated ~0.9, pentacoordinated ~1.1, hexacoordinated ~1.2 mm s^{-1}. The absorption and the line width values are highly dependent on the temperature and the nature of the substituent. The crystal structure of the complex $[Fe(DMTU)_6](BF_4)_2$·DMTU was determined by heavy-atom methods and refined by least-squares procedures. Crystals are monoclinic, space group $C2/c$, with $a = 13.561$ (3) Å, $b = 24.008$ (4) Å, $c = 14.290$ (4) Å, $\beta = 91.36$ (2)°, and $Z = 4$, and the structure was refined to $R = 0.045$ for the 3037 independent reflections greater than 3σ.

Introduction

The structure and bonding of Fe–S compounds have been of interest to us for some years.[1-9] The use of Fe–S compounds as models for iron–sulfur proteins has been pursued by many groups for many years.[10-12] Although there has been much work with Fe(III) complexed with dithiocarbamates and thioxanthates,[13-18] there has been relatively little work on Fe(II) in general and Fe(II) complexes with soft, neutral ligands in particular.

There is some indirect structural information obtained from Mössbauer spectroscopy for iron(II) complexes with substituted thioureas. It has been possible to observe considerable distortion in the crystal field symmetry from that expected for regular

* To whom correspondence should be addressed.
† Texas A&M University.
‡ Studies performed at Case Institute of Technology, Cleveland, OH.
§ Universidad de Santiago.
‖ Universidad de Chile.
⊥ Present address: Department of Chemistry, Universidad de La Frontera, Temuco, Chile.

(1) Fackler, J. P.; Coucouvanis, D. *Proc. Int. Conf. Coord. Chem., 9th* **1966**, 300.
(2) Fackler, J. P.; Holah, D. G. *Inorg. Nucl. Chem. Lett.* **1966**, *2*, 251.
(3) Fackler, J. P.; Seidel, W. C. *Inorg. Chem.* **1969**, *8*, 1631.
(4) Fackler, J. P.; Lin, I. J. B.; Andrews, J. *Inorg. Chem.* **1977**, *16*, 450.
(5) Fackler, J. P.; Thompson, L. D., Jr. *Inorg. Chim. Acta* **1981**, *48*, 45. This paper describes refinement procedures used.
(6) Latorre, R.; Abeledo, C.; Costamagna, J.; Frankel, R.; Reiff, W.; Frank, E. *J. Chem. Phys.* **1973**, *59*, 2580.
(7) Latorre, R.; Costamagna, J.; Frank, E.; Abeledo, C.; Frankel, R. *J. Phys. C* **1974**, *12*, C6-635.
(8) Latorre, R.; Costamagna, J.; Frank, E.; Abeledo, C.; Frankel, R. *J. Inorg. Nucl. Chem.* **1979**, *41*, 649.
(9) Latorre, R.; Costamagna, J.; Navia, P. *J. Phys. C* **1976**, *14*, C6-489.
(10) For a review of this subject, see: (a) Malkin, R.; Rabinowitz, S. J. C. *Annu. Rev. Biochem.* **1967**, *36*, 113. (b) Kimura, T. *Struct. Bonding (Berlin)* **1968**, *5*, 1. (c) Tribi, J. C. M.; Woody, R. W. *Coord. Chem. Rev.* **1970**, *5*, 417.

0020-1669/87/1326-0836$01.50/0